Egyptian Journal of Chemistry

Electronic Cigarettes Flavoring Chemicals: Theoretical Insights on Reactivities, Bond Dissociation Energy and Photophysical Characteristics

Mohamed Sabry Ahmed Abdel-Mottaleb[a*] and Yousra Abdel-Mottaleb[b]

[a] Department of Chemistry, Computational Chemistry Lab, Faculty of Science, Ain Shams University, 11566 Abbassia, Cairo, Egypt
[b] Department of Pharmacology, Toxicology, and Biochemistry, Faculty of Pharmaceutical Sciences and Pharmaceutical Industries, Future University in Egypt (FUE), 11835 Cairo, Egypt

Abstract

We investigated the molecular electronic structure characteristics of flavoring chemicals 2,3-butanedione (**1**) and the analog 2,3-pentanedione (**2**) and its reduced form acetoin (**3**) within DFT. The study includes estimating essential issues of their interactions such as the chemical reactivity, bond dissociation energy (BDE), and potential energy curves (PES) of COCO homolytic bond rupture. Relaxed scanning of the ground state geometry at different theory levels generated PES for S_0, S_1, S_2, T_1 and T_2 states. Based on the excited state dynamic (ESD) module of the ORCA package, we predicted the excited states' radiative (fluorescence and phosphorescence) and non-radiative (intersystem crossing (ISC)) emission rates to provide a detailed picture of the considered flavors' photophysical characteristics. The information gained could be helpful for ongoing investigations on the toxicity, health, and environmental impact of the vaporizations and free-radical formation of foods and E-cigarettes' flavors. It may represent a practical orientation for assessing the effectiveness of flavors' safety for the health and the atmosphere and predicting more stable candidates.

Keywords: α-Diketones; DFT; Bond Dissociation Energy; reactivity indices; deactivation rates

1. Introduction

Electronic cigarette (e-cig) use has increased too quickly worldwide over the last decade due to a penetrating marketing promotion aiming to push them to reduce or eliminate the habit of tobacco cigarette smoke [1]. Moreover, a provocative debate is still ongoing within the scientific community on possible effects on both users' and bystanders' health. There are significant anxieties about e-cig use related obviously to e-liquids composition. Some problems are the possible breath exposure to flavors present in the preparations and the potential exposure to harmful by-products formed during the vaporization and the dissociation process [2-5]. Given the health-related worries raised by the international scientific community and EU member states' experienced authorities, specific requirements concerning e-cigs manufacture were incorporated in the EU Tobacco Products Directive 2014/40/EU (TPD) [6].

Our attention here is focused on the intrinsic properties and photophysical characteristics of e-cig-based alpha-diketones and their structurally related acetoin (α-hydroxy ketone).

The simplicity of 2,3-butanedione, 2,3-pentanedione, and acetoin makes them suitable model molecules to study various characteristics (Figure 1).
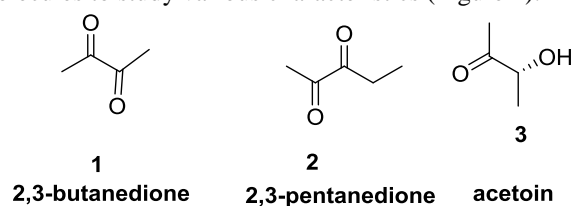

Figure 1. The 2D structures of the studied molecules

It is well known that naturally occurred or chemically produced molecules **1**, **2**, and **3** are popular flavorants in the food industry. They are made during the coffee roasting process [7]. Recent studies discovered a connection between the flavors and bronchiolitis obliterans, known as "popcorn lung," a disease first detected in workers at popcorn factories

_____

[8]. Furthermore, they are also released during the composting of solid wastes and digestates [9].

A hot investigation has evaluated the effect of the flavoring chemicals on human bronchial epithelial cells in culture and proposed a possible mechanism for how they could impair lung function [10]. Few ongoing studies are investigating the health impacts of these compounds on e-cigarette users [11]. Chemical toxicity is often associated with the covalent modification of cellular nucleophiles by electrophilic chemicals. Electrophilic α-diketones may covalently modify nucleophilic arginine residues in critical proteins and, thereby, produce the observed respiratory-tract pathology. The major pathway for the biotransformation of α-diketones is reducing to α-hydroxyketones (acyloins) [12,13]. For this reason, we will predict the reactivity indices of these molecules from the energies of their frontier orbitals.

Additionally, because of its impact on the atmosphere, few studies were reported on pyrolysis, photolysis, dissociation, fragmentation, and DFT investigations of mainly 2,3-butanedione (diacetyl) (**1**) and 2,3-pentanedione (**2**). [14 – 19]. One of the sources of atmospheric free-radicals is from the pyrolysis and photolysis of alpha-diketones. The generated free radicals interact with the atmospheric hydroxyl radical and ozone. Thus, these flavors' thermal stability is an essential issue for environmental impacts and health concerns, so we will investigate further to shed light on the free radical generation by pyrolysis and photolysis.

Despite its intrinsic interest and practical importance, the triplet state interactions and phosphorescence have seemed far removed from more commonly studied physical and chemical properties [20-27]. The primary missing information concerns the photophysical characteristics. Therefore, one final goal of this work is to attempt to supply some of the missing information. We here report that a theoretical study of phosphorescence provides quantitative data on the alpha diketones and acetoin triplet state involved in chemical reactions considered a source for harmful free-radical productions.

2. Computations.

All calculations were carried out, exploiting the ORCA 4.2 (parallel) software package [28]. We applied density functional theory (DFT) and its time-dependent extension (TD-DFT) and employing the range-separated hybrid functional ω B97X-3D [29,30] that includes empirical corrections for long-range non-bonded dispersive interactions and basis set 6-311G(d,p). This is one of the recommended methods for the geometries of organic molecules. Overlap fitted RIJCOSX approximation was used to improve the calculations' efficiency and enhance speedups at almost no harm. [31]. We utilized the CPCM solvation model with acetonitrile [32].
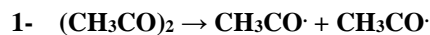
The rates and spectra were calculated using the same methods recommended and detailed in the literature [33, 34], employing the "ESD module" in the Orca program package. When computing phosphorescence rates k_{Phos}, each rate was requested individually. For the flavours under investigation, we were predicted the k_{Phos} as the mean of the sum of the individual k_{Phos} (T_1), k_{Phos} (T_2), and k_{Phos} (T_3). When indicating k_{ISC}, we also considered the triplet spin-sublevels (1, 0, or -1), and the k_{ISC} is the sum of the individuals.
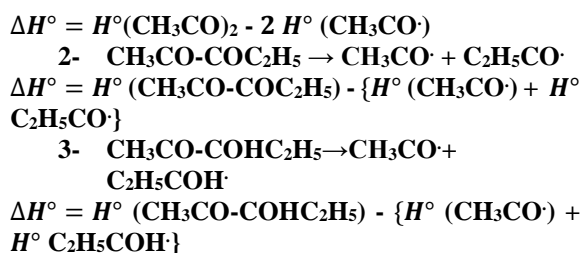
Dissociation of the COCO was studied via relaxed linear transit scan using TDDFT as implemented in the Orca program package, changing CO-CO distance from 1.0 to 3.0 Å in 30 steps. Potential energy curves of the ground and excited states of the molecules were evaluated. Moreover, to overcome the failure of the PES at a more considerable distance, we employed the Iterative-Configuration Expansion Configuration Interaction (ICE-CI) method of the ORCA package [28]. The ICE-CI advantage is that the potential energy surface is entirely smooth and correctly behaves in the dissociation limit. The calculation utilizes the basis: def2-SVPD [35, 36]. Our calculation utilizes the auxiliary basis: def2-SVP/C [37]. Potential energy curves of the ground and excited singlets and the triplet states of the molecules were evaluated separately and added to the same figure.

3. Results and Discussion

3.1. Bond Dissociation Energy (BDE).

The flavors' thermal stability is an important issue to investigate to shed light on the free radical generation by pyrolysis and photolysis. Information acquired from previous studies confirms homolytic bond dissociation as the first step in molecular degradation. The fragmentation pattern obtained from Mass spectroscopic studies [https://webbook.nist.gov/cgi/cbook.cgi?ID=C431038&Mask=200#] reveals a dominant fragment 43 m/e in the spectrum of diacetyl, which corresponds to acetyl species CH3CO due to homolytic dissociation of diacetyl1. Two dominant fragments at 43 and 57 m/e correspond to the existence of CH3CO and CH3CH2CO species in the case of 2. This finding confirms that the primary step in the fragmentation of both molecules is the COCO bond dissociation. This prompted us to compute CO-CO bond dissociation energy in the three compounds and compare our results with the reported BDE. The BDE is given in terms of enthalpy change (ΔH°) of the dissociation reactions below according to the following equations:

1- (CH₃CO)₂ → CH₃CO· + CH₃CO·

_____

$\Delta H° = H°(CH_3CO)_2 - 2 H° (CH_3CO·)$

2- $CH_3CO\text{-}COC_2H_5 \rightarrow CH_3CO· + C_2H_5CO·$

$\Delta H° = H° (CH_3CO\text{-}COC_2H_5) - \{H° (CH_3CO·) + H° C_2H_5CO·\}$

3- $CH_3CO\text{-}COHC_2H_5 \rightarrow CH_3CO·+ C_2H_5COH·$

$\Delta H° = H° (CH_3CO\text{-}COHC_2H_5) - \{H° (CH_3CO·) + H° C_2H_5COH·\}$

Our computed results are summarized in Table 1. Excellent agreements with the experimentally reported data could be noticed by inspection of Table 1, revealing that our simple theoretical methodology is adequate for validating the experimental data. It could be safely used to predict accurately enough BDE for other structurally related flavors.

Another possible way to predict BDE is by scanning along the distance between the two carbonyl groups to get the potential energy surface (PES). We met difficulties generating PES regarding inconsistent quality throughout the surface at distances more considerable than the equilibrium minimum. In other words, the description of the bond did not remain consistent along with all spaces by the method we used. In section 3.3. we are going to illustrate and fix the issue further.

Table 1. Thermodynamic parameters and the predicted and the available experimental BDE (kcal/mol) of the flavors and the corresponding radicals. Observed values are reported in [15-19, 38]

Molecule	Energy (au)	H° (au)	G° (au)			
1	-306.475	-306.378	-306.413			
2	-345.79	-345.665	-345.704			
3	-306.475	-306.378	-306.413			
Radical	Energy (au)	H° (au)	G° (au)	BDE ΔE	BDE ΔH	BDE Exp.
1·	-153.18	-153.134	-153.164	-72.53	-69.58	-66.9 – -72.9
2·	-192.495	-192.42	-192.455	-72.26	-69.56	-67.9
3·	-154.375	-154.307	-154.338	-75.04	-71.32	--

Finally, rate constants for the volatile hydroxy carbonyls' reactions with OH and NO_3 radicals and O_3 have been reported [39]. The NO_3 radical and O_3 reactions are slow. The OH radical reactions will be the dominant atmospheric gas-phase loss process for these hydroxy carbonyls, within general, calculated lifetimes for the OH radical reactions of 0.7-1.5 days [39]. However, to the best of our knowledge, no details exist on the bond dissociation's reactions generated radicals of the flavors with the OH, NO_3, or O_3 radicals in the atmosphere.

3.2. Reactivity Indices

Reactivity indices were defined and discussed in [40], reflect the electronic changes induced by substituents in a closely related series of molecules. Molecular reactivity indices such as chemical potential (μ), hardness (η), and electrophilicity (ω), were calculated from the energies of frontier orbitals and defined as follows:

(1) Chemical potential is simply defined as μ=0.5(LUMO+HOMO)

(2) Hardness is given by η=0.5(LUMO-HOMO)

The chemical hardness η can be believed of as a molecule's resistance to exchange electron density with other molecules. Softness is, however, the reciprocal of hardness.

(3) Electrophilicity is given by $ω=μ^2/2η$, which measures a molecule's ability to attract electrons. The electrophilicity index measures a molecule's energy stabilization if it acquires an additional electron density from the environment. The electrophilicity index is considered a crucial parameter for studying the reactivity of a series of molecules.

Our computed results reveal the close similarities between 1 and 2, while the parameters are drastically different for 3. Acetoin 3 has the smallest ω value and is a weaker electron acceptor relative to diacetyl1 or 2,3-pentadione 2. Also, it is much harder (η = 5.13) to release electrons than 1 and 2. Thus, it is expected that both 1 and 2 should have closely similar electronic characteristics that will reflect on their photophysical parameters.

Table 2. The frontier orbital energies and the reactivity indices (in eV) defined in [40] for the flavors.

Molecule	HOMO	LUMO	μ	η	ω
1	-9.09	-0.54	-4.82	4.28	2.71
2	-9.02	-0.48	-4.75	4.27	2.64
3	-9.02	1.23	-3.90	5.13	1.48

Similar conclusions have been reached in studying the toxicity of diacetyl 1 and related α-diketone 2 and its reduced form the acetoin 3 [12,13]. The reduction of α-diketones to the less electrophilic acyloins is a detoxication pathway for α-diketones.

Excited-state Photophysics.
3.1.1. Potential energy surfaces.
We generated Figure 2 (see figure caption) to fundamentally test PESs in different excited states for conical intersections that could be responsible for radiationless deactivations processes, including the intersystem crossing,
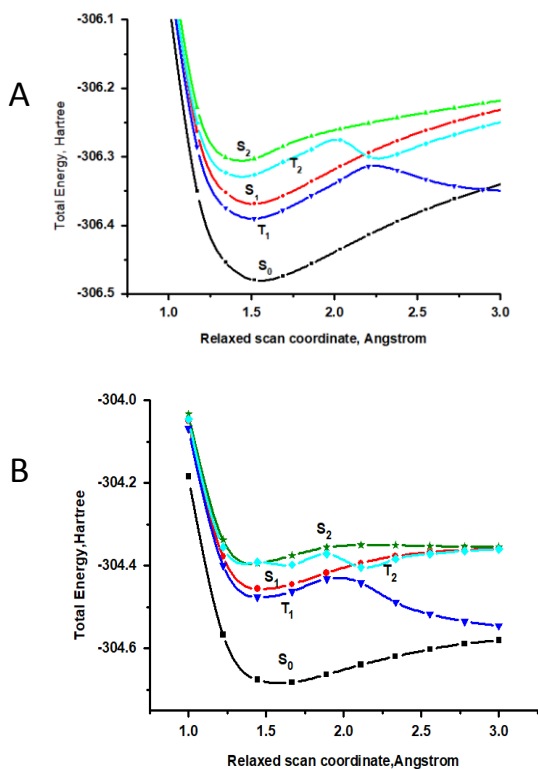

Figure 2. PES curves of different excited states of molecule 1. C-C bond distance of COCO is the scan coordinate. Similar PES curves were obtained for 2 and 3. Curves A shows an intersection between the T1 (blue) and the S0 (black) at 2.85 Angstrom *Curve B obtained by the computationally expensive ICE-CI method showing no intersection between the T_1 (blue) and the S_0 (black) at 2.85 Angstrom.*

Figure 2 shows several points of intersections between the PESs of the singlets and triplet states. This is entirely happening, as shown between the T1 and S$_0$, because at above 2 Angstrom apart, the nature of the scanned distance changes. Consequently, BDE cannot be produced from the PES. Fortunately, ORCA features a method that has been termed Iterative-Configuration Expansion Configuration Interaction (ICE-CI) [28]. The ICE-CI goal is to provide compact wavefunction(s) (e.g., one or several states) close to the full-CI limit at a reasonable enough computational cost. We used ICE-CI to scan all potential energy surfaces, as presented in Figure 2 (B). From the vertical difference between the equilibrium distance and the curve at 3.0 Angstrom, we get the BDE value of equal -64.0 kcal/mol for 1 and 2, which is in good agreement with the experimental amount listed in Table 2. A value of -72.5 kcal/mol was obtained for 3 because the reduction of 1 resulted in a stronger COCOH bond relative to the COCO bond, which suffers from the electron withdrawings' properties of the two carbonyls oxygen. In general, the non-parallelity error along a potential energy surface is, to a large extent, avoided. Thus, ICE-CI yields consistent quality throughout the surface. Hence, the description of the bond remains constant to a large extent. The PES is entirely smooth and also correctly behaves in the dissociation limit. Figure 2 (B) shows that near the minimum, it is very close to the applied method represented in Figure 2 (A) that T1 drops below the S0 state as the bond is stretched.

3.1.2. Excited-state decay kinetics
We observed an overall similarity in the flavors' absorption and luminescence spectra. The wavelength of maximum emission of fluorescence and phosphorescence varies only slightly with increased chain length or the hydroxyl group [41]. The most crucial difference is the intensity of the phosphorescence peaks. Figure 3 shows the predicted phosphorescence and absorption spectra of **1** in acetonitrile as an example (molecules **2** and **3** have similar spectra, see Table 3). Predicted and experimental spectral band positions are in satisfactory agreement (see Table 3).

In liquid solution at around 25°C, there is a decreasing phosphorescence intensity in the order **1** > **2** > **3**, validating the experimental observations [16, 41]. This effect is shown to be due to the increased probability of fluorescence or radiationless deactivation with increasing chain length or hydroxyl group instead of the alpha carbonyl one. It was reported that all the aliphatic α- diketones are suitable acceptors in triplet-triplet energy transfer [16, 41]. Studies on the products of the gas-phase reactions of selected flavors with OH radicals, NO$_3$ radicals, and

O$_3$ under atmospheric conditions seems to be missing, as discussed in section 3.1.
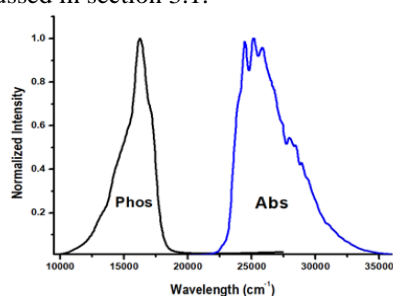

Figure 3. The predicted phosphorescence and absorption spectra of molecule 1 in acetonitrile.

We then carried out excited-state dynamic computations to predict the triplet state's photophysical characteristics of molecules 3 and 2. We then compared the results with that of 1 to consider the effect of the alpha-hydroxyl group in 3 and the substitution of a hydrogen atom by the methyl group in the case of 2 on the radiationless processes in these flavors.

Table 3. Photophysical data of the flavors studied. The phosphorescence lifetime ($1/ k_{phos}/s^{-1}$) is given between parenthesis in ms. (Available experimental data are provided [20, 41] *)

Molecule	phos/nm	Abs/nm	k_f/s^{-1}	k_{phos}/s^{-1}	k_{ISC}/s^{-1}
1	604.4 {520} *	470 {422} *	0.924 e+5	190 (5.26)	7.83 e+5
2	543.4 {500} *	465.8 {419} *	1.01 e+5	150 (6.67)	1.398 e+5
3	421.0	311.0	2.88 e+5	35 (28.57)	15.77 e+7

*Experimental data of 1 and 2 in ethyl ether-isopentane-ethanol (5:5:2 volume ratio) [41].

The effect on the deactivation rates of the excited state of molecular architecture is summarized in Figure 4. Molecule **2** fluoresces somewhat faster and is of marginally lower k_{ISC} and k_{Phos} than **1**. Alpha-hydroxy ketone (acetoin **3**) exhibits remarkable fluorescence and intersystem crossing rates over those of **1**. In conclusion, the triplet state lifetime in **3** is relatively long; a condition considerably favors triplet state interaction than in **1** and **2**.
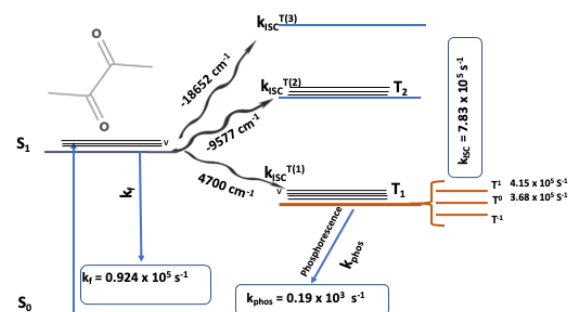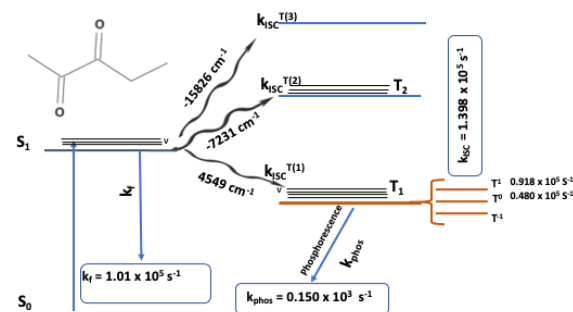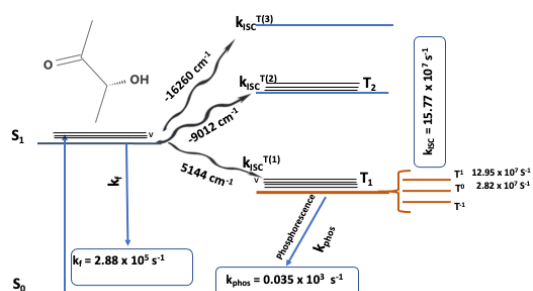

Figure 4. Scheme for calculating photophysical processes in 1, 2, and 3 (from bottom to top, respectively). The $k_{ISC}(i)$ between the S$_1$ and T$_1$ is the sum of the transitions to the spin-sublevels indicated as T$_1$ and T$_0$. The k_{ISC} to T$_2$ and T$_3$ are negligible.

Thus, it is highly expected that the excited states' radiationless processes play a dominant role in the studied flavors' photophysics. Therefore, these molecules are not astonishing to populate their triplet states, leading to the observed phosphorescence at room temperature.

4. Conclusion

We predicted the reactivity indices, the BDE, and the photophysical properties of three flavors for food and e-cigarettes, negatively impacting human health and the atmosphere. Generally, excellent agreement with the available experimental data was achieved. Toxicity is related to the electrophilicity of the molecules. The acetoin is less reactive and less toxic than the other two alpha-diketones based on the electrophilicity index. PES of the S$_0$ obtained by applying the ICE-CI method yields BDE value in good agreement with the experimental value. The triplet state lifetime and the predicted bond dissociation energy point to the possibility of free radical generation due to smoking and vaporization of the flavors. The studied flavors' molecular structure is reflected in the predicted rates of radiative (k_{Flu} and k_{Phos}) and non-radiative processes (k_{ISC}). The reduced form of diacetyl 1, the acetoin, has the highest ISC and

_____

fluorescence rate and the lowest phosphorescent rate relative to the two alpha-diketones 1 and 2.

Consequently, its triplet-state is more inert relative to the alpha-diketones studied. The information gained could be helpful for the ongoing examinations on the health and environmental impact of the vaporizations and free-radical formation of foods and E-cigarettes' flavors. It may represent a practical orientation for assessing the effectiveness of flavors' safety for the health and the atmosphere and predicting more stable candidates.

References
1. M. Dockrell, R. Morrison, L. Bauld, A. McNeill. E-cigarettes: prevalence and attitudes in Great Britain. Nicotine Tob. Res. 15 (2013) 1737–1744.
2. M. Famele, J. Palmisani, C. Ferranti, C. Abenavoli, L. Palleschi, R. Mancinelli, R. M. Fidente, G. De Gennaro, R. Draisci, Liquid chromatography with tandem mass spectrometry method for the determination of nicotine and minor tobacco alkaloids in electronic cigarette refill liquids and second-hand generated aerosol. J. Sep. Sci. 40 (2017) 1049–1056
3. O. Geiss, I. Bianchi, F. Barahona, J. Barrero-Moreno, Characterisation of mainstream and passive vapors emitted by selected electronic cigarettes. Int. J. Hyg. Environ. Health 218 (2015) 169–180
4. J. W. Flora, N. Meruva, C. B. Huang, C. T. Wilkinson, R. Ballentine, D. C. Smith, M. S. Werley, W. J. McKinney, Characterization of potential impurities and degradation products in electronic cigarette formulations and aerosols. Regul. Toxicol. Pharmacol. 74 (2016) 1–11
5. E. E. Omaiye, K. J. McWhirter, W. Luo, P. A. Tierney, J. F. Pankow, P. Talbot, High concentrations of flavor chemicals are present in electronic cigarette refill fluids. Sci. Rep. 2468 (2019) 1-9
6. European Parliament. Directive 2014/40/EU of the European Parliament and of the Council of 3 April 2014 on the Approximation of the Laws, Regulations and Administrative Provisions of the Member States Concerning the Manufacture, Presentation and Sale of Tobacco and Related Products and Repealing Directive 2001/37/EC; European Parliament: Brussels, Belgium, 2014. http://data.europa.eu/eli/dir/2014/40/oj
7. M. Daglia, A. Papetti, P. Grisoli, C. Aceti, V. Spini, C. Dacarro, G. Gazzani, Isolation, identification, and quantification of roasted coffee antibacterial compounds, J Agric Food Chem. 55 (2007) 10208-13
8. (National Institute for Occupational Safety and Health)
9. C. A. Rincón, Amaury De Guardia, Annabelle Couvert, SophieL, RouxaI sabelle Soutrel, Mylène Daumoin, Jean Claude Benoist, Chemical and odor characterization of gas emissions released during composting of solid wastes and digestates, Journal of Environmental Management, 233 (2019) 39-53
10. Hae-Ryung Park et al., Transcriptomic response of primary human airway epithelial cells to flavoring chemicals in electronic cigarettes, Scientific Reports 9(1):1400, DOI:10.1038/s41598-018-37913-9
11. (https://cen.acs.org/biological-chemistry/genomics/Two-common-flavoring-chemicals-e/97/web/2019/02?utm_source=Newsletter&utm_medium=Newsletter&utm_campaign=CEN&referral=BBB98285-F27D-433A-82BE-DF5477799000).
12. M W Anders, Diacetyl and related flavorant α-Diketones: Biotransformation, cellular interactions, and respiratory-tract toxicity, Toxicology, 2017, 388, 21-29, DOI: 10.1016/j.tox.2017.02.002
13. R. M. Lo Pachin, Terrence Gavin, Anthony De Caprio, and David S. Barber
    Application of the Hard and Soft, Acids, and Bases (HSAB) Theory to Toxicant Target Interactions, dx.doi.org/10.1021/tx2003257 | Chem. Res. Toxicol. 2012, 25, 239–251].
14. C. N. Plum, Eugenio. Sanhueza, Roger. Atkinson, William P. L. Carter, and James N. Pitts, Hydroxyl radical rate constants and photolysis rates of alpha-dicarbonyls, Environ. Sci. Technol. 17 (1983) 479–484.
15. X. L. Yang, A. W. Jasper, J. H. Kiefer, R. S. Tranter, The Dissociation of Diacetyl: A Shock Tube and Theoretical Study, J. Phys. Chem. A, 113 (2009) 8318 – 8326
16. B. Klotz et al., A kinetic study of the atmospheric photolysis of α-dicarbonyls, International Journal of Chemical Kinetics, 33 (2001) 9-20.
17. E. Murad, M. G. Inghram, Thermodynamic properties of the acetyl radical and bond dissociation energies in aliphatic carbonyl compounds, J. Chem. Phys., 41 (1964) 404.
18. A. Gomez-Zavaglia, and R. Fausto, Matrix-isolation and solid-state low temperature FT-IR study of 2,3-butanedione (diacetyl), Journal of Molecular Structure 195 (2003) 661-662
19. K. Scherzer, D. Plarre, Der Thermische Zerfall von Diacetyl, II. Mitteilung: Untersuchungen bei

_____

hohen Temperaturen, Z. Phys. Chem. (Leipzig), 256 (1975) 668

20. H. H. Richtol and F. H. Klappmeier, luminescence and energy transfer in some aliphatic α- diketones, J. Chem. Phys. 44 (1966) 1519 – 1523.

21. Gilbert N. Lewis and M. Kasha, Phosphorescence and the Triplet State, J. Am. Chem. Soc. 1944, 66, 12, 2100–2116

22. Max S. Matheson and J. William Zabor, Fluorescence of Carbonyl Compounds in the Gas Phase, J. Chem. Phys. 7 (1939) 536

23. A. W. Jackson and a. J. Yarwood, Radiation and radiationless processes in 2,3-pentanedione; phosphorescence lifetime in the gas phase, Canadian journal of Chemistry, 49 (1971) 987-993

24. J. Heicklen, The Fluorescence and Phosphorescence of Biacetyl Vapor and Acetone Vapor, J. Am. Chem. Soc. 81 (1959) 3863–3866

25. M. Almgren, the natural phosphorescence lifetime of biacetyl and benzil in fluid solution, 6 (1967) 829-840

26. H. Okabe and W. Albert Noyes Jr., The Relative Intensities of Fluorescence and Phosphorescence in Biacetyl Vapor, J. Am. Chem. Soc. 79 (1957) 801–806, https://doi.org/10.1021/ja01561a006

27. J. T. Dubois and B. Stevens, Luminescence of Organic and Inorganic Materials. John Wiley & Sons, Inc., New York, 1962

28. F. Neese, The ORCA program system Wiley interdisciplinary Reviews - Computational Molecular Science, 2 (2012) 73-78; ORCA4.2. And the Manual at https://orcaforum.kofo.mpg.de/

29. A. Jaoul, G. Nocton, C. Clavaguera, Assessment of Density Functionals for Computing Thermodynamic Properties of Lanthanide Complexes, ChemPhysChem, 18 (2017) 2688 – 2696.

30. D. J. Chai, M. Head-Gordon, Systematic optimization of long-range corrected hybrid density functionals, J. Chem. Phys. 128 (2008) 084106.

31. F. Neese, F. Wennmohs, A. Hansen, U. Becker, Efficient, approximate and parallel Hartree-Fock and hybrid DFT calculations. A 'chain-of-spheres' algorithm for the Hartree-Fock exchange, Chem. Phys. 356 (2009) 98- 109.

32. M. Cossi, N. Rega, G. Scalmani, V. Barone, Energies, Structures, and Electronic Properties of Molecules in Solution with the C-PCM Solvation Model, J. Comput. Chem. 24 (2003) 669 - 681.

33. B. de Souza, F. Neese, R. Izsák, On the theoretical prediction of fluorescence rates from first principles using the path integral approach. J. Chem. Phys. 148 (2018) 34104 https://doi.org/10.1063/1.5010895]

34. B. de Souza, G. Farias, F. Neese, and R. Izsák, Predicting Phosphorescence Rates of Light Organic Molecules Using Time-Dependent Density Functional Theory and the Path Integral Approach to Dynamics J. Chem. Theory Comput. 15 (2019) 1896–1904.

35. F Weigend and R. Ahlrichs, Balanced basis sets of split valence, triple zeta valence and quadruple zeta valence quality for H to Rn: Design and assessment of accuracy, Phys. Chem. Chem. Phys. 7 (2005) 3297 – 3305.

36. D. Rappoport and F. Furche, Property-optimized Gaussian basis sets for molecular response calculations, J. Chem. Phys. 133 (2010) 134105.

37. A. Hellweg, C. Hattig, S. Hofener and W. Klopper, Optimized accurate auxiliary basis sets for RI-MP2 and RI-CC2 calculations for the atoms Rb to Rn, Theor. Chem. Acc. 117 (2007) 587 – 597.

38. Sidney W. Benson, III - Bond energies, J. Chem. Educ. 42 (1965) 502-518.

39. Sara M. Aschmann, Janet Arey, and Roger Atkinson, Atmospheric Chemistry of Selected Hydroxycarbonyls, J. Phys. Chem. A 104 (2000) 3998–4003. https://doi.org/10.1021/jp9939874https://cfpub.epa.gov/ncer_abstracts/index.cfm/fuseaction/display.abstractDetail/abstract/700/report/F

40. F. Zielinskim V. Tognetti, L. Joubert, Condensed descriptors for reactivity: A methodological study. Chem Phys Lett. 527 (2012) 67 – 72.

41. T. R. Evans and Peter A. Leermakers, Emission Spectra and Excited-State Geometry of a-Diketones, J. Am. Chem. Soc. 89 (1967) 4380–4382.